Motion Modeling and Deployment Control of a Long Tethered Spacecraft System with an Atmospheric Sounder

Zhe Dong, Yuriy M. Zabolotnov, and Changqing Wang

***Abstract*—The paper studies the deployment dynamics of a long tethered spacecraft system (TSS) with an atmospheric sounder. The tether (several ten kilometers) is deployed from the spacecraft by means of a mechanism that works only for braking. A dynamic nominal deployment control law is designed in an orbital moving coordinate system taking into account the aerodynamic forces acting on the end-bodies (the spacecraft and atmospheric sounder) and inextensible tether. The motion stability of the TSS is analyzed. The deployment process is studied in a geocentric coordinate system with consideration of the dynamics of control mechanism operation, tether elasticity, and other perturbations. The numerical simulations show that designing the nominal deployment control law taking into account the aerodynamic force reduces the system's control error several times for the deployment process.**

***Index Terms*—Tethered spacecraft system, atmospheric sounder, modeling, nominal deployment control law, motion stability, control error**

I. Introduction

In recent years, tethered spacecraft systems (TSSs) have received much attention for a number of applications such as tether-assisted re-entry [1, 2], active debris removal and deorbiting [3 – 7], planetary exploration [8] and atmospheric sounding [9 – 11]. Generally, there are three dynamic phases for a typical TSS space mission: deployment, station-keeping, and retrieval [12]. Among these three phases, the deployment phase is the premise of a successful space mission, because the flexible TSS would exhibit an unstable motion during the deployment process if without control [13–15].

Many researchers have paid attention to the deployment control of the TSS for a number of occasions. The long TSS (the tether length is of the order of several ten kilometers) should be considered as a system with distributed parameters, and its motion is generally described by partial differential equations. The system with distributed parameters makes the control problem complicated [16, 17]. As a result of this, various simplified models of the motion of the TSS have been used to design control laws. In these simplified models the tether is treated as a massless/massive rigid rod [18 – 21]. A validation model is used to provide more detailed insight into the system dynamics and to test the control laws [18, 22]. The flexibility and extensibility of the tether and the dynamics of the control mechanism operation are considered in the validation model. The tether is considered as a sequence of elements, such as beads connected by massless springs, lumped masses connected by massless springs-dashpot, a series of rigid rods, or finite elements in the validation model [23].

The most important external perturbation for the low orbital non-conductive TSS is the aerodynamic force [11, 24]. The stability of the stationary state of the TSS with an atmospheric sounder has been studied in detail in the classical monograph [9]. As shown in the monograph [9], there is an air-gradient instability position during the motion of the TSS. The air-gradient instability is shown as an increase in the swing amplitude with respect to the equilibrium position of the system. In addition to this, if the tether length is smaller than a critical value, the swing of the TSS will be constrained. Based on the study of the oscillations of a spacecraft with a spacecraft with a vertical tethered system under the action of the gravitational moment and small periodic tethered force at a circular orbit [25], the gravitational stabilization of the relative equilibrium position of the STS in a circular orbit is studied in [26]. The swing of a movable mass solves the problem of the gravitational stabilization.

The atmospheric sounder in this paper is a kind of light metallic and inflatable structure, and its shape is close to sphere. The ballistic coefficient ($\sigma = c_x S / m$, where c_x is the drag coefficient of the object, S is the cross-sectional area of the object in the direction of the object's motion relative to the atmosphere, m is the object's mass) of the atmospheric sounder is relatively large. The cross-sectional area of the tether is calculated by $S_t = D_t L$ (D_t is the diameter of the tether, L is the tether length) if the tether length is of the order of several ten kilometers. It turns out that the cross-sectional area of the tether is much larger than the cross-sectional areas of the end-bodies. This leads to the necessity of taking into account the aerodynamic force acting on the tether when we design the nominal deployment control law.

To the best knowledge of the authors, taking into account

Manuscript received April 02, 2018; This work was supported by CSC (China Scholarship Council), the Fundamental Research Funds for the Central Universities (3102017JC06002) and Shaanxi science and technology program (2017KW-ZD-04).

Zhe Dong is with the Informatics Department, Samara National Research University, Samara, 443086 Russia (e-mail: dongzhe@yandex.ru).

Yuriy M. Zabolotnov is with the Informatics Department, Samara National Research University, Samara, 443086 Russia (e-mail: yumz@yandex.ru).

Changqing Wang is with the Department of Automation, Northwestern Polytechnical University, Xi'an, 710072 China (e-mail: wangcq@nwpu.edu.cn).

the aerodynamic force acting on the components of the TSS (the spacecraft, the atmospheric sounder and the tether) for designing the nominal deployment control law has not been considered. Therefore, in this paper a simplified motion model of the TSS taking into account the aerodynamic force acting on the components of the TSS is used for obtaining the motion stability condition for the initial deployment phase and designing the dynamic deployment control law. The dynamic deployment control law in this paper generalizes the control laws, which have been used in [9, 18, 27].

A more complex motion model of the TSS is used for estimating the applicability of the proposed nominal deployment control law. In the complex model the tether is treated as a sequence of point masses with one-sided elastic mechanical coupling. A linear feedback controller in terms of the errors in the tether length and deployment rate is used. The tether deployment mechanism in this work, which can just brake the tether, is similar to the mechanism that was used in the space tethered experiment YES2 [19, 28]. The numerical simulations show that the proposed nominal deployment control law can significantly reduce the control error and swing amplitude of the TSS with respect to the equilibrium position.

II. Mathematical Model for Designing Nominal Control Law

The coordinate systems $OXYZ$, $OX_oY_oZ_o$, $Cx_oy_oz_o$, $Cx_ty_tz_t$ (see Fig. 1 and Fig. 2) are used for deriving the motion equations of the TSS. The geocentric right-hand coordinate system $OXYZ$ is associated with the orbital plane of the system center of mass C, where axis OX is in the direction along the nodal line, and axis OZ is in the direction of the angular momentum vector of the orbital motion. The geocentric orbital moving coordinate system $OX_oY_oZ_o$ rotates with respect to the coordinate system $OXYZ$ with the angular velocity $\Omega = d\gamma / dt$, where γ is the argument of latitude. The axes of the coordinate systems $OX_oY_oZ_o$ and $Cx_oy_oz_o$ are parallel (see Fig. 1), and the only difference between these two coordinate systems is in the coordinates of the origin. The coordinate system $Cx_ty_tz_t$ is associated with the tether and axis Cx_t is directed along the tether. The relative positions of the coordinate systems $Cx_ty_tz_t$ and $Cx_oy_oz_o$ are described by angles θ and β (see Fig. 2).

The following assumptions are made for developing the simplified model of the TSS: 1) the orbit of the system center of mass is unchanged and nearly a circular orbit during the deployment; 2) the tether is deployed from the spacecraft; 3) the extensibility and flexibility of the tether are neglected; 4) the spacecraft and atmospheric sounder are regarded as the point masses; 5) the tether is treated as a rigid massive rod.

The motion equations of the TSS for designing the nominal deployment control law are derived in [27] without taking into account the aerodynamic force acting on the TSS. The equations are derived from the Lagrangian equation with the generalized coordinates $q_1 = L$, $q_2 = \theta$, $q_3 = \beta$, where L is the tether length.

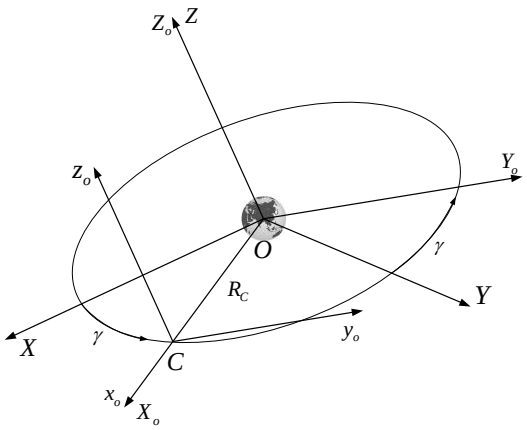

Fig. 1 Coordinate systems.

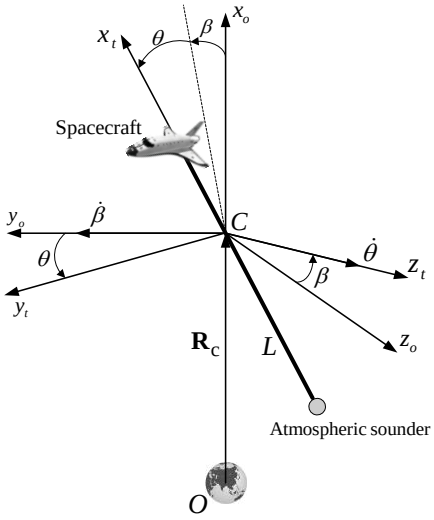

Fig. 2 Relative positions of coordinate systems $Cx_oy_oz_o$ and $Cx_ty_tz_t$.

In this paper the motion equations of the TSS taking into account the aerodynamic forces acting on the spacecraft, atmospheric sounder and tether are presented as:

$$\ddot{L} = \frac{\nu_e}{M_e} L T_1 + \frac{Q_L - T_p}{M_e}, \tag{1}$$

$$\ddot{\theta} = -2\frac{\nu_e}{J_e} L \dot{L}(\dot{\theta} + \Omega\cos\beta) + T_2 + \frac{Q_\theta}{J_e}, \tag{2}$$

$$\begin{aligned}\ddot{\beta}\cos^2\theta = &-2\frac{\nu_e}{J_e} L \dot{L}(\dot{\beta}\cos^2\theta + \Omega\sin 2\theta\sin\beta) \\ &+ T_3 + \frac{Q_\beta}{J_e}\end{aligned}, \tag{3}$$

where

$$\begin{aligned}T_1 = &\dot{\theta}^2 + 2\Omega\dot{\theta}\cos\beta + \dot{\beta}^2\cos^2\theta - \Omega^2\cos^2\theta\sin^2\beta \\ &+ \Omega\dot{\beta}\sin\beta\sin 2\theta + 3\Omega^2\cos^2\theta\cos^2\beta\end{aligned}, \tag{4}$$

$$\begin{aligned}T_2 = &\Omega^2\sin\theta\cos\theta\sin^2\beta - \dot{\beta}^2\sin\theta\cos\theta \\ &+ 2\Omega\dot{\beta}\cos^2\theta\sin\beta - \frac{3}{2}\Omega^2\sin 2\theta\cos^2\beta\end{aligned}, \tag{5}$$

$$T_3 = \dot{\theta}\dot{\beta}\sin 2\theta - 2\Omega\dot{\theta}\cos^2\theta\sin\beta - 2L^2\Omega^2\cos^2\theta\sin 2\beta, \quad (6)$$

$$\nu_e = \frac{(m_1^0 - L\rho_t)(m_n + L\rho_t/2)}{M}, \quad (7)$$

$$M_e = \frac{(m_1^0 - L\rho_t)(m_n + L\rho_t)}{M}, \quad (8)$$

$$J_e = \frac{L^2}{12M}(12m_1^0 m_n - 8L\rho_t m_n + 4L\rho_t m_1^0 - 3L^2\rho_t{}^2), \quad (9)$$

where m_1^0 is the initial mass of the spacecraft, m_n is the mass of the atmospheric sounder, ρ_t is the line density of the tether material, $M = m_1^0 + m_n$, T_p is the nominal tensional force of the tether, Q_L, Q_θ, Q_β are the generalized aerodynamic forces.

The equations of the plane motion ($\beta = 0$) are used for designing the nominal control law for the TSS deployment into the vertical position:

$$\ddot{L} = \frac{\nu_e}{M_e}L[(\dot{\theta}+\Omega)^2 - \Omega^2(1-3\cos^2\theta)] + \frac{Q_L - T_p}{M_e}, \quad (10)$$

$$\ddot{\theta} = -2\frac{\nu_e}{J_e}L\dot{L}(\dot{\theta}+\Omega) - \frac{3}{2}\Omega^2\sin 2\theta + \frac{Q_\theta}{J_e}. \quad (11)$$

Additionally, in order to verify the assumption that the orbit of the system center of mass is unchanged and nearly a circular orbit during the deployment, the change in the orbital altitude of the system center of mass is taken into account [29]:

$$\dot{V}_c = \frac{R_{cv}}{M} - \mu\frac{\sin\vartheta}{(R_3+H_c)^2}, \quad (12)$$

$$\dot{\vartheta} = \frac{R_{cn}}{MV_c} - \left[\frac{\mu}{(R_3+H_c)^2} - \frac{V_c^2}{R_3+H_c}\right]\frac{\cos\vartheta}{V_c}, \quad (13)$$

$$\dot{H}_c = V_c\sin\vartheta, \quad (14)$$

where μ is the Earth's gravitational parameter, V_c, H_c are the velocity and orbital altitude of the system center of mass, respectively, ϑ is the inclination angle of the trajectory of the system center of mass (angle between the local horizon and the velocity of the system center of mass), R_3 is the mean radius of the Earth, R_{cv} is the projection of the resultant aerodynamic force on the direction of the velocity of the system center of mass, R_{cn} is the projection of the resultant aerodynamic force on the normal direction of the trajectory plane of the system center of mass.

The generalized aerodynamic forces are defined with the expressions $Q_L = \delta W_L/\delta L$, $Q_\theta = \delta W_\theta/\delta\theta$, where δW_L and δW_θ are the virtual works over the displacements δL and $\delta\theta$, respectively. The generalized aerodynamic forces for the TSS are calculated as:

$$Q_\theta = Q_{\theta 1} + Q_{\theta n} + Q_{\theta t},\ Q_L = Q_{L1} + Q_{Ln} + Q_{Lt}, \quad (15)$$

where $Q_{\theta 1}$, Q_{L1} and $Q_{\theta n}$, Q_{Ln} are the generalized aerodynamic forces for the spacecraft and atmospheric sounder (1 denotes the spacecraft, *n* denotes the atmospheric sounder). $Q_{\theta t}$ and Q_{Lt} are the generalized aerodynamic forces for the tether.

The generalized aerodynamic forces for the spacecraft and atmospheric sounder are calculated as [30]:

$$Q_{\theta 1} = -\frac{1}{2}c_1 S_1\rho_1 V_1 L_1(V_{e1}\cos(\theta-\varphi_1) + V_{\theta 1}), \quad (16)$$

$$Q_{\theta n} = \frac{1}{2}c_n S_n\rho_n V_n L_n(V_{en}\cos(\theta+\varphi_n) - V_{\theta n}), \quad (17)$$

$$Q_{L1} = -\frac{1}{2M}c_1 S_1\rho_1 V_1\left(m_n + \frac{L\rho_t}{2}\right) \cdot (V_{e1}\sin(\theta-\varphi_1) + V_{L1}), \quad (18)$$

$$Q_{Ln} = \frac{1}{2M}c_n S_n\rho_n V_n\left(m_1^0 - L\rho_t/2\right) \cdot (V_{en}\sin(\theta+\varphi_n) - V_{Ln}), \quad (19)$$

where $V_{\theta k} = L_k\dot{\theta}$, $V_{Lk} = \dot{L}_k$ ($k = 1, n$), $L_1 = L(m_n + L\rho_t/2)/M$, $L_n = L(m_1^0 - L\rho_t/2)/M$, V_{ek} are the velocities of the end-bodies due to the rotation of the coordinate system $OX_oY_oZ_o$, S_k are the cross-sectional areas of the end-bodies in the direction of the motion of the end-bodies relative to the atmosphere, c_k are the drag coefficients, ρ_k are the atmospheric densities, V_k are the velocity modules. φ_k are the angles between the radius vector of the system center of mass $\mathbf{R}_c$ and the radius vectors of the end-bodies in $OX_oY_oZ_o$.

The generalized aerodynamic force for the tether is calculated by the integration over the tether length under the assumption that the tether is straight:

$$Q_{\theta t} = \int_0^L R_{tl}l_x|\sin\alpha_t|dx,\ Q_{Lt} = \int_0^L R_{tl}\cos\alpha_t dx, \quad (20)$$

where $R_{tl} = \frac{1}{2}c_t\rho D_t V_t^2|\sin\alpha_t|$ is the aerodynamic force acting on an element of the tether, D_t and c_t are the diameter and drag coefficient of the tether, α_t and V_t are the angle of attack and velocity module of the tether element, $l_x = L_n - x$ is the moment arm of the aerodynamic force acting on the tether element with respect to the system center of mass. The calculation of the integral is implemented by discretizing the tether into elements and then summating. The direction of the aerodynamic force acting on the tether element is opposite to the resultant velocity of the tether element's center of mass, i.e. assume that the TSS's motion occurs in a free molecular flow, and the hypothesis on the diffuse reflection of molecules is used [31].

The atmospheric density ρ is calculated based on the standard atmosphere parameters of GOST 25645.101–83 [32]. The integration for (20) is approached by a 5th degree interpolation polynomial. The rotation of the atmosphere is neglected for designing the nominal deployment control law.

III. Nominal deployment control law

The nominal control law for the TSS deployment into the vertical position is designed under the conditions of the system's motion at the end of the deployment $\dot{L} = \ddot{L} = 0$, $L = L_{\text{end}}$, where L_{end} is the total tether length. Equations (10 – 11) will have the equilibrium position $\theta = \theta_1$ ($\dot{\theta} = \ddot{\theta} = 0$), which is near the local vertical, if the tensional force is determined from the expression:

$$T_p = \nu_e \Omega^2 \cos^2\theta_1 [a(L - L_{\text{end}}) + \frac{b\dot{L}}{\Omega} + 3L_{\text{end}}] + Q_L, \quad (21)$$

where a and b are the parameters of the control law, θ_1 is the deflection angle of the tether from the local vertical, which is determined from (11) for $\dot{\theta} = \ddot{\theta} = \dot{L} = 0$.

If $a > 3$, $b > 0$ and the changes in the orbital parameters are neglected, then (10 – 11) will have an asymptotic stable equilibrium position $\theta = \theta_1$, $L = L_{\text{end}}$, $\dot{\theta} = \ddot{\theta} = \dot{L} = \ddot{L} = 0$. The demonstration of this conclusion is given in [18, 27], which is carried out by analyzing the eigenvalues of the corresponding linearized system. In addition to this, there exist some critical values b_* ($b_* > 0$) for the parameter b when $a = \text{const}$. All eigenvalues of the linearized system become negative when $b > b_*$. In this case, $\dot{L} > 0$, $\ddot{L} < 0$, $L < L_{\text{end}}$ are satisfied due to the asymptotic stability. The satisfaction of these restrictions is a necessary condition for designing the nominal deployment control law, because it is assumed that the tether deployment mechanism works only for braking and cannot pull the tether. On the other hand, when the values of the parameters a and b are close to the critical values $a = a_* = 3$, $b = b_*$, the deployment time decreases. This can be an additional criterion for selecting the values of parameters a and b.

IV. Analysis of motion stability of TSS

The motion stability includes the stability of the equilibrium position of the TSS near the local vertical (static stability) and deployment stability (dynamic stability). The dynamic stability and static stability are analyzed with the assumption $\dot{L} \neq 0$ and $L = \text{const}$, respectively. The TSS may lose the motion stability due to the aerodynamic force if the deflection angle of the tether from the local vertical is larger than $\pi/2$. The loss of motion stability may cause the collision of the spacecraft and atmospheric sounder, the tether slack and tether twining, which directly affect the flight safety of the TSS.

The following assumptions are adopted for the approximate analysis of the motion stability:

$$\varphi_k \approx \varphi_{tx} \approx 0, \; V_{Lk} << V_k, \; V_{\theta k} << V_k, \; V_{\theta tx} << V_{tx}, \quad (22)$$

where $k = 1, n$, φ_{tx} is the angle between $\mathbf{R}_c$ and the radius vector of the center of the tether element, $V_{\theta tx} = L_{tx}\dot{\theta}$, L_{tx} is the linear distance between the center of the tether element and the system center of mass, V_{tx} is the velocity module of the tether element. The angles $\varphi_k \approx \varphi_{tx} \approx 0$ when the tether length is of the order of several ten kilometers. The relative velocities V_{Lk}, $V_{\theta k}$, $V_{\theta tx}$ are smaller than 0.1% of the orbital motion velocities V_k and V_{tx}. Additionally, $V_k \approx V_{tx} \approx V_c$, where $V_c = \Omega R_c$ is the orbital velocity of the system center of mass.

Equation (11) is presented in the non-dimensional form by adopting the assumptions (22):

$$\theta'' + \frac{3}{2}\sin 2\theta + F(\theta, \nu, \xi) = 0, \quad (23)$$

where $\theta'' = \frac{d^2\theta}{d\tau^2}$, $\tau = \Omega t$ is the non-dimensional time,

$$F(\theta, \nu, \xi) = \nu \cos\theta + \xi \cos^2\theta, \quad (24)$$

$$\nu = \frac{V_c^2 L}{2J_e\Omega^2}(c_1 S_1 \rho_1 \frac{m_n + L\rho_t/2}{M} - c_n S_n \rho_n \frac{m_1^0 - L\rho_t/2}{M}), \quad (25)$$

$$\xi = \frac{\int_0^L c_t \rho D_t l_x R_c^2 dx}{2J_e}. \quad (26)$$

The energy integral for (23) is presented as:

$$\frac{(\theta')^2}{2} + P(\theta, \nu, \xi) = E = \text{const}, \quad (27)$$

where

$$P(\theta, \nu, \xi) = -\frac{3}{4}\cos 2\theta + \nu \sin\theta + \xi(\frac{\theta}{2} + \frac{1}{4}\sin 2\theta), \quad (28)$$

$P(\theta, \nu, \xi)$ is the analogue potential energy of the TSS.

According to the Lagrange-Dirichlet theory, the equilibrium point of the TSS is stable if the TSS's potential energy has a strict local minimum on this equilibrium point, and is unstable if maximum. Based on this, the singular points of the TSS corresponding to (23) are presented in Table I, where $\varphi = \arcsin(\xi/\sqrt{9+\xi^2})$.

TABLE I
Singular points (θ) of TSS

ν	$\nu < -3$	$\nu \in (-3, 3)$	$\nu > 3$
Stable points	$\pi/2$	$-\arcsin(\nu/\sqrt{9+\xi^2}) - \varphi$, $\pi + \arcsin(\nu/\sqrt{9+\xi^2}) + \varphi$	$3\pi/2$
Unstable points	$3\pi/2$	$\pi/2$, $3\pi/2$	$\pi/2$

According to Table I, if $\nu \in (-3, 3)$, then the TSS has two stable equilibrium positions near the local vertical. In addition to this, the values and signs of the shifts of the stable equilibrium positions with respect to the local vertical depends on ν. If $|\nu| > 3$, then the stable equilibrium positions of the TSS are horizontal.

Therefore, the condition of static stability of the TSS is presented as:

$$|\nu| < 3. \quad (29)$$

If the condition (29) is always satisfied, then it can be regarded as the necessary condition of the deployment motion

stability of the TSS.

Fig. 3 shows the phase trajectory corresponding to (23) when $\nu = -1.5$. In this case, there are two static stable equilibrium positions near the local vertical.

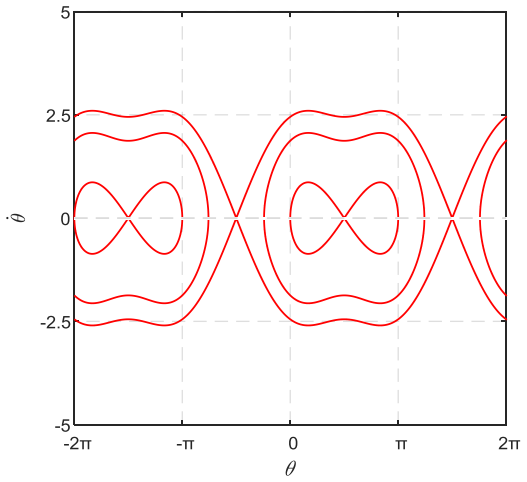

Fig. 3 Phase trajectory corresponding to (23) ($\nu = -1.5$)

The non-dimensional parameters ν and ξ represent the ratios between the aerodynamic moment and the gravitational moment of the end-bodies and tether, respectively. The dynamic stability of the system with respect to the equilibrium position, which is close to the local vertical, is determined by $F(\theta, \nu, \xi)$. $F(\theta, \nu, \xi)$ depends on the changes in the parameters of the TSS during the deployment. In addition, the influence of $F(\theta, \nu, \xi)$ will increase if the tether length is small due to the features of the parameters ν and ξ. In addition to this, the gravitational moment tends to be zero when $L \to 0$. Therefore, the analysis of dynamic stability of the TSS deserves special attention paid to the initial deployment phase, which immediately follows the separation between the spacecraft and atmospheric sounder.

The analysis of the initial deployment phase of the TSS shows that there are two characteristic cases. The difference between these two cases is the sign of ν. The signs of the parameters ν and ξ correspond to the sign of the aerodynamic moment with respect to the system center of mass. On the other hand, the moment due to the Coriolis force always points in one direction during the deployment ($\dot{L} > 0$). The direction of the moment due to the Coriolis force is opposite to the direction of the angular velocity of the system center of mass ($\mathbf{\Omega}$). Therefore, the most dangerous case from the point-of-view of losing the motion stability of the TSS is that the signs of the parameters ν and ξ are the same, and the direction of the moment due to the Coriolis force coincides with the signs of ν and ξ.

The orbital altitudes of the spacecraft and atmospheric sounder are almost the same in the initial deployment phase. Therefore, $\rho_1 = \rho_n$. According to this, the sign and value of ν are presented as an interval of the ballistic coefficient $\Delta\sigma = \sigma_1 - (\sigma_n + \sigma_t)$, where σ_1, σ_n, σ_t are the ballistic coefficients of the spacecraft, atmospheric sounder and tether, respectively. In this case, the sufficient condition of the motion stability of the TSS is presented as:

$$\Delta\sigma_1 < \Delta\sigma < \Delta\sigma_2, \tag{30}$$

where $\Delta\sigma_1 < 0$, $\Delta\sigma_2 < 0$, $|\Delta\sigma_2| < |\Delta\sigma_1|$. The interval of $\Delta\sigma$ is asymmetrical, because the moment due to the Coriolis force always points in one direction during the deployment. The boundary values of $\Delta\sigma$ can be obtained only numerically if the parameters of the TSS are known. For example, if the mass of the atmospheric sounder is $m_n = 5\,\text{kg}$, other parameters used for calculation are presented in Table II. The boundary values of $\Delta\sigma$ can be obtained by means of changing the cross-sectional area of the atmospheric sounder: $\Delta\sigma_1 = -37.69\,\text{m}^2/\text{kg}$, $\Delta\sigma_2 = -0.45\,\text{m}^2/\text{kg}$.

TABLE II
PARAMETERS OF TSS (A)

Parameter	Value	Unit
Initial altitude of circular orbit: H_c	270	km
Total tether length: L_{end}	30	km
Line density of tether material: ρ_t	0.2	kg/km
Tether diameter: D_t	0.6	mm
Drag coefficients of the spacecraft and atmospheric sounder: c_k ($k = 1, n$)	2.4	
Drag coefficient of the tether: c_t	2.2	
Relative velocity of separating atmospheric sounder from spacecraft along the local vertical downward: ΔV_r	2	m/s
Cross-sectional area of the spacecraft: S_1	3.14	m^2
Ballistic coefficient of the spacecraft: σ_1	$3\cdot10^{-3}$	m^2/kg
Initial mass of the spacecraft: m_1^0	2500	kg
Parameter of the control law: a	4	
Parameter of the control law: b	5	

If the structure of the atmospheric sounder is lightweight and foldable (or an inflatable balloon), the effect of the aerodynamic force on the initial deployment phase can be reduced. Firstly, the atmospheric sounder is kept compressed in the initial deployment phase and then the atmospheric sounder will be unfolded (or the inflatable balloon will be aerated) after passing the dangerous initial phase. The time for keeping the atmospheric sounder foldable can be calculated according to (30).

V. ANALYSIS OF NOMINAL DEPLOYMENT TRAJECTORIES OF TSS

The comparison of the nominal deployment trajectories by using the nominal control law (21) is shown in this section. The comparison is between the nominal deployment trajectories with and without taking into account the aerodynamic forces acting on the spacecraft, atmospheric sounder and tether. The diameter and mass of the atmospheric sounder for the numerical simulations in this section are 1 m and 20 kg, respectively.

The nominal trajectories of the atmospheric sounder with

respect to the spacecraft with and without taking into account the contribution of the aerodynamic force are shown in Fig. 4. It is shown that for the case of taking into account the aerodynamic force the sign of the deflection angle of the tether from the local vertical changes at the end of the deployment.

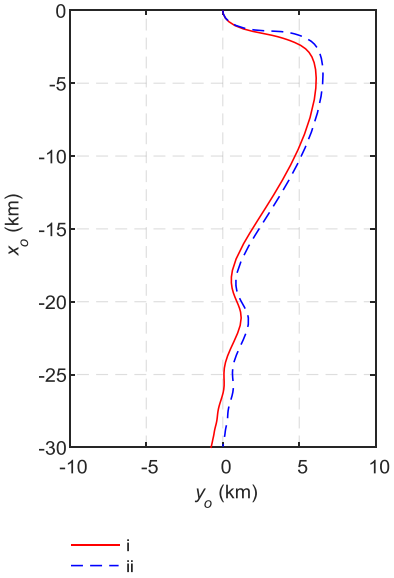

Fig. 4 Nominal trajectories of the atmospheric sounder with respect to the spacecraft: (i) with consideration of the aerodynamic force, (ii) without consideration of the aerodynamic force.

This corresponds to the increase in the braking force (tensional force) when the aerodynamic force is taken into account (see Fig. 5), where $\tau = t / t_p$ is the non-dimensional time, t_p is the period of motion of the system on the initial circular orbit.

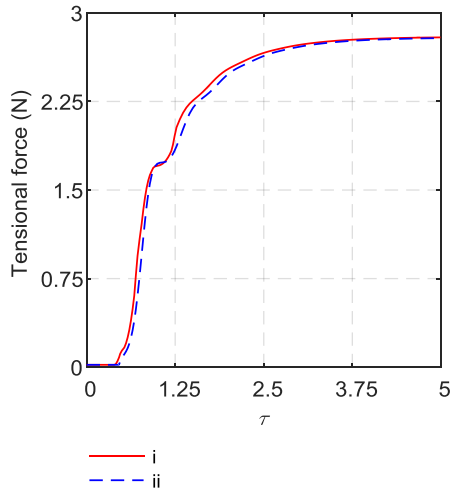

Fig. 5 Tensional force: (i) with consideration of the aerodynamic force, (ii) without consideration of the aerodynamic force.

The increase in the braking force makes the decelerating phase of the deployment process start earlier (see Fig. 6). Fig. 6 shows the deployment rate with and without taking into account the aerodynamic force. The deployment process consists of the accelerating and decelerating phases. At the end of the deployment the condition $\dot{L} = 0$ is satisfied. The aerodynamic forces acting on the spacecraft (R_1), atmospheric sounder (R_n) and tether (R_t) are shown in Fig. 7. It is shown that the aerodynamic force acting on the tether is much larger than the aerodynamic forces acting on the spacecraft and atmospheric sounder even though the tether's diameter for simulation is relatively small ($D_t = 0.6$ mm). During the deployment process the changes in the orbital altitude and angular velocity of the system center of mass are less than 2 km and $1 \cdot 10^{-6}$ s^{-1}, respectively.

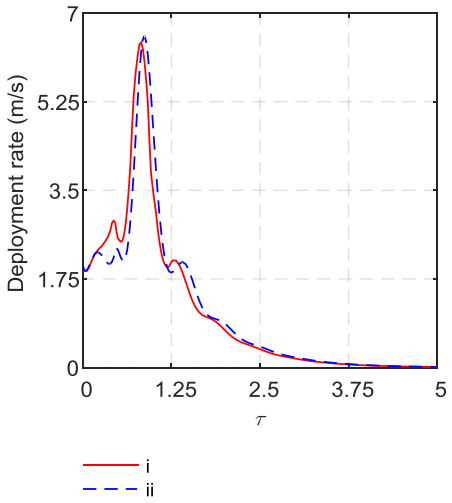

Fig. 6 Deployment rate: (i) with consideration of the aerodynamic force, (ii) without consideration of the aerodynamic force.

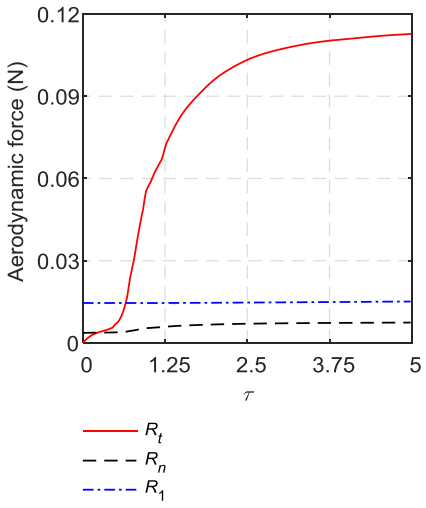

Fig. 7 Aerodynamic forces acting on the spacecraft (R_1), atmospheric sounder (R_n) and tether (R_t).

VI. Mathematical Model with Distributed Parameters for Validation

A discrete model of motion is used to estimate the applicability of the nominal deployment control law (21). The motion model with distributed parameters is developed in the geocentric right-hand coordinate system $OXYZ$. In this model the TSS is considered as n point masses with one-sided elastic mechanical coupling (see Fig. 8).

The motion equations of the TSS taking into account the aerodynamic force are presented as [33]:

$$\frac{d\mathbf{r}_j}{dt}=\mathbf{V}_j,\ m_j\frac{d\mathbf{V}_j}{dt}=\mathbf{G}_j+\mathbf{T}_j-\mathbf{T}_{j-1}+\mathbf{R}_j, \quad (31)$$

where $\mathbf{r}_j$ ($j=1,2,...,n$) are the positions of the spacecraft ($j=1$), point masses of the tether ($j=2,3,...,n-1$) and atmospheric sounder ($j=n$), $m_j=m_t/(n-2)$ ($j=2,3,...,n-1$) are the tether's point mass, m_t is the tether's mass, n is the number of the TSS's point masses, $\mathbf{V}_j$ is the absolute velocity, $\mathbf{G}_j$ is the gravitational force, $\mathbf{R}_j$ is the aerodynamic force.

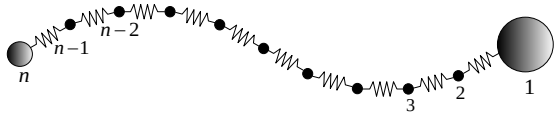

Fig. 8 Model with distributed parameters for TSS.

The tensional force $\mathbf{T}_j$ is calculated according to the Hooke's law taking into account that the mechanical coupling is one-sided:

$$\mathbf{T}_j=T_j\frac{\mathbf{r}_{j+1}-\mathbf{r}_j}{\left|\mathbf{r}_{j+1}-\mathbf{r}_j\right|},\ \left(j=1,2,...,n-1\right) \quad (32)$$

$$T_j=\begin{cases}c\dfrac{\left|\mathbf{r}_{j+1}-\mathbf{r}_j\right|-\Delta L_j}{\Delta L_j} & \left(\left|\mathbf{r}_j-\mathbf{r}_{j+1}\right|-\Delta L_j\ge 0\right)\\ 0 & \left(\left|\mathbf{r}_j-\mathbf{r}_{j+1}\right|-\Delta L_j<0\right)\end{cases}, \quad (33)$$

where ΔL_j is the unstrained length of the tether element, c is the stiffness of the tether. In addition, only one tensional force acts on the end-bodies, i.e. $\mathbf{T}_0=\mathbf{T}_n=0$.

The gravitational force is calculated as:

$$\mathbf{G}_j=-\mu\frac{m_j\mathbf{r}_j}{r_j^3},\ \left(j=1,2,...,n\right) \quad (34)$$

The aerodynamic force acting on the tether element is calculated as:

$$\mathbf{R}_{c,j}=-\frac{1}{2}c_t\rho D_t\Delta L_j V_{c,j}\mathbf{V}_{c,j}\left|\sin(\alpha_j)\right|, \quad (35)$$

where $\mathbf{V}_{c,j}$ ($j=1,2,...,n-1$) is the velocity of the center of tether element with respect to the atmosphere, α_j is the angle of attack of the tether element.

$\mathbf{V}_{c,j}$ and α_j are calculated as:

$$\mathbf{V}_{c,j}=\frac{\mathbf{V}_{r,j}+\mathbf{V}_{r,j+1}}{2}, \quad (36)$$

$$\cos\alpha_j=\frac{\left(\mathbf{r}_{j+1}-\mathbf{r}_j\right)\cdot\mathbf{V}_{c,j}}{\left|\mathbf{r}_{j+1}-\mathbf{r}_j\right|V_{c,j}}, \quad (37)$$

where $\mathbf{V}_{r,j}$ is the velocity of the tether's point mass with respect to the atmosphere.

The aerodynamic forces acting on the tether's point masses and end-bodies are calculated as:

$$\mathbf{R}_j=\frac{\mathbf{R}_{c,j-1}+\mathbf{R}_{c,j}}{2},\ (j=2,3,...,n-1) \quad (38)$$

$$\mathbf{R}_1=-\frac{1}{2}c_1\rho_1 S_1\left|\mathbf{V}_{r,1}\right|\mathbf{V}_{r,1}+\frac{\mathbf{R}_{c,1}}{2}, \quad (39)$$

$$\mathbf{R}_n=-\frac{1}{2}c_n\rho_n S_n\left|\mathbf{V}_{r,n}\right|\mathbf{V}_{r,n}+\frac{\mathbf{R}_{c,n-1}}{2}. \quad (40)$$

The relationship between the absolute and relative velocities is presented as:

$$\mathbf{V}_{r,j}=\mathbf{V}_j-\boldsymbol{\Omega}_e\times\mathbf{r}_j,\ (j=1,2,...,n) \quad (41)$$

where $\boldsymbol{\Omega}_e$ is the angular velocity of the Earth's self-rotation.

The motion equation (31) is associated with the equation that takes into account the dynamics of the control mechanism operation. The latter can be described as [18, 27]:

$$m_e\frac{dV_l}{dt}=T_1-F_c,\ \frac{dl}{dt}=V_l, \quad (42)$$

where the coefficient m_e describes the inertia of the control mechanism (it is assumed that $m_e=\text{const}$ during the deployment process), l is the unstrained length of the tether deployed from the control mechanism, V_l is the deployment rate.

According to the feedback principle, F_c is presented as [19]:

$$F_c=T_p+p_1\Delta_1+p_2\Delta_2, \quad (43)$$

where $\Delta_1=l-L$, $\Delta_2=V_l-\dot{L}$, p_1 and p_2 are the feedback coefficients, T_p is the nominal tensional force determined in (21), L and $\dot{L}$ are the nominal values determined in (10 – 11). The limitation $F_c\ge F_{\min}$ is considered for calculating (43). The sampling step of the controller is taken into account in this paper.

The momentum conservation principle is used at the moment of separating the atmospheric sounder from the spacecraft. The absolute velocities of the spacecraft and atmospheric sounder are calculated as:

$$\mathbf{V}_1=\mathbf{V}_c-\frac{m_n}{M}\Delta\mathbf{V}_r,\ \mathbf{V}_n=\mathbf{V}_1+\Delta\mathbf{V}_r, \quad (44)$$

where $\Delta\mathbf{V}_r$ is the relative velocity of separating the atmospheric sounder from the spacecraft along the local vertical downward. $\mathbf{V}_c$ is the absolute velocity of the system center of mass before separation.

The dimension of motion model (31) increases during the deployment process, as it is necessary to add new point masses due to the continual increase in the tether length [18].

VII. Analysis of Deployment Dynamics of TSS

The parameters used for numerical simulations in this section are presented in Table II and Table III. The values of the feedback coefficients (p_1, p_2) can ensure the stability of the deployment process [18]. The sampling step $h=0.01\,\text{s}$. The sampling step describes the time interval of the deployment control mechanism output, i.e. the output of the deployment control mechanism updates every h seconds.

TABLE III
PARAMETERS OF TSS (B)

Parameter	Value	Unit
Inertia of control mechanism: m_e	0.2	kg
Stiffness of the tether: c	7070	N
Minimum control force for deployment mechanism: $F_{\min}$	0.01	N
Feedback coefficient: p_1	0.243	kg/s^2
Feedback coefficient: p_2	7.824	kg/s

The trajectories of the atmospheric sounder with respect to the spacecraft are shown in Fig. 9. The control force of the deployment mechanism and the nominal control force are shown in Fig. 10. Fig. 11 and Fig. 12 show the control errors in the tether length and deployment rate. Fig. 9(a), Fig. 10(a), Fig. 11(a) and Fig. 12(a) correspond to the case without consideration of the aerodynamic force for determining the nominal variables $L(t)$ and $\dot{L}(t)$. Fig. 9(b), Fig. 10(b), Fig. 11(b) and Fig. 12(b) correspond to the case taking into account the contribution of the aerodynamic force. The results of numerical simulations show that using the nominal deployment control law without taking into account the aerodynamic force leads to the large control errors in bringing the atmospheric sounder into the local vertical (see Fig. 10(a), Fig. 11(a) and Fig. 12(a)). This control error causes a large swing amplitude with respect to the local vertical (see Fig. 9(a)). Taking into account the aerodynamic force for designing the nominal control law dramatically reduces the swing amplitude (see Fig. 9(b)) and control errors (see Fig. 10(b), Fig. 11(b) and Fig. 12(b)). In this case, the swing amplitude with respect to the local vertical is reduced approximately 3 times, as shown in Figure 9. The swing of the TSS is caused by the joint effect of the gravitational and aerodynamic forces [9]. The change in the orbital altitude of the system center of mass is also less than 2 km.

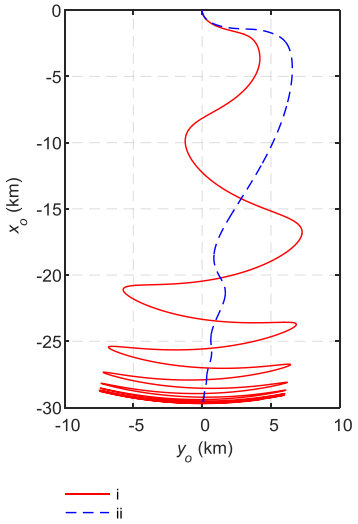

(a)

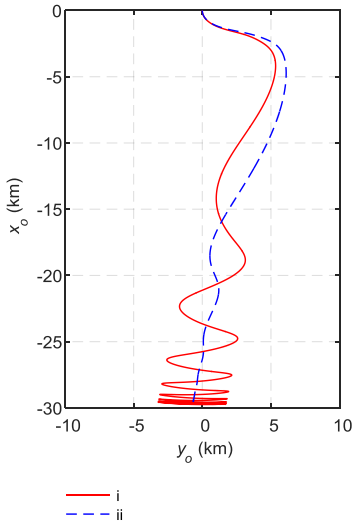

(b)

Fig. 9 Trajectories of the atmospheric sounder with respect to the spacecraft (i – perturbed trajectory; ii – nominal trajectory): (a) without consideration of the aerodynamic force; (b) with consideration of the aerodynamic force.

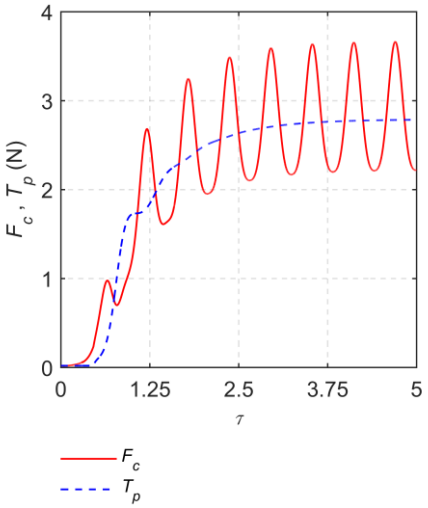

(a)

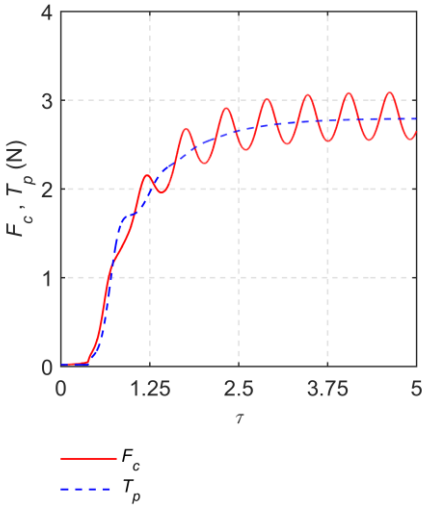

(b)

Fig. 10 Control force of the deployment mechanism (F_c) and nominal control force (T_p): (a) without consideration of the aerodynamic force; (b) with consideration of the aerodynamic force.

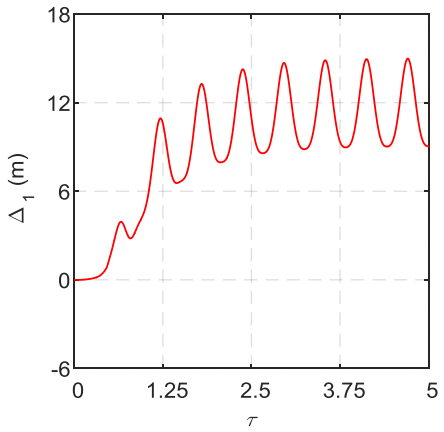

(a)

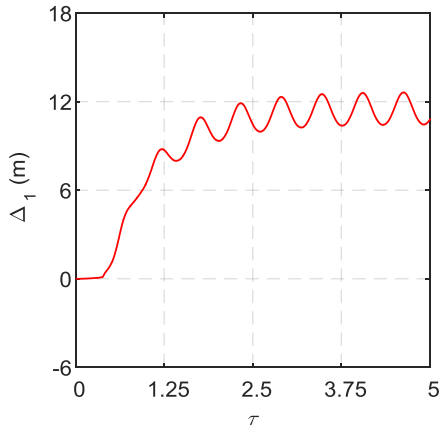

(b)

Fig. 11 Control error in the tether length: (a) without consideration of the aerodynamic force; (b) with consideration of the aerodynamic force.

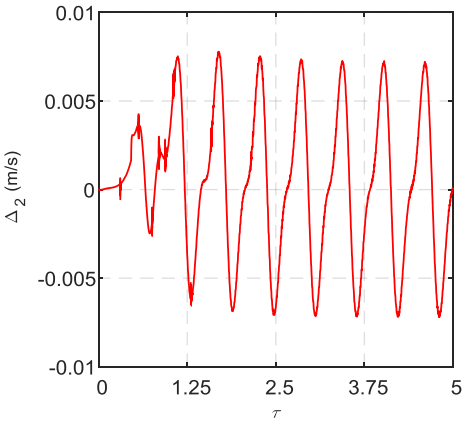

(a)

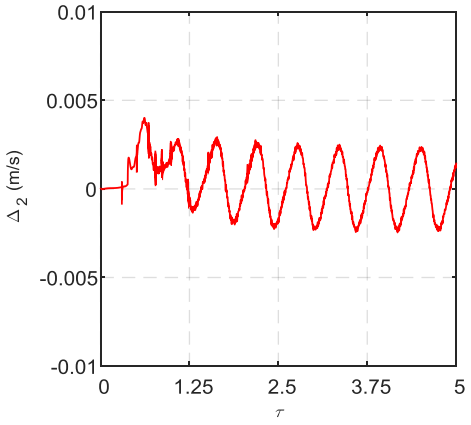

(b)

Fig. 12 Control error in the deployment rate: (a) without consideration of the aerodynamic force; (b) with consideration of the aerodynamic force.

The comparison of the swing amplitude with respect to the local vertical for various altitudes of the circular orbit (H_c) and tether lengths is shown in Table IV.

TABLE IV
SWING AMPLITUDE WITH RESPECT TO THE LOCAL VERTICAL (KM):
1 – WITHOUT CONSIDERATION OF THE AERODYNAMIC FORCE
2 –WITH CONSIDERATION OF THE AERODYNAMIC FORCE

L_{end} (km)	$H_c = 250$ km		$H_c = 270$ km		$H_c = 300$ km	
	1	2	1	2	1	2
20	3.89	0.74	3.26	0.55	2.31	0.44
30	6.84	2.33	6.71	2.31	5.91	2.25
40	7.31	4.43	7.78	4.88	7.95	4.91

The simulation results in Table IV show that the swing amplitude decreases for all cases considered in this paper if the nominal deployment control law is designed taking into account the aerodynamic force. However, the effectiveness of the proposed nominal control law decreases with the increase in the tether length. In addition to this, if the total tether length $L_{\text{end}} > 60$ km , using the proposed nominal control law cannot reduce the control errors or swing amplitude in bringing the atmospheric sounder into the local vertical.

For the case that the masses of the spacecraft and atmospheric sounder are comparable, for example, $m_1^0 = 100$ kg , $m_n = 20$ kg , the results in Table IV change very little. However, in this case, the change in the orbital altitude of the system center of mass becomes larger due to the increase in the ballistic coefficient of the spacecraft.

The assessment of the influence of the sampling step on the control process quality is shown in Table V. Table V shows the comparison of the swing amplitude (A) for various sampling steps h .

The numerical results in Table V show that the increase in the sampling step leads to the increase in the swing amplitude with respect to the local vertical. However, there is a range for h . In this range the swing amplitude are approximately constant. The range for the numerical results in Table V is $h \in [0.01\,\text{s}, 0.04\,\text{s}]$. If $h > 0.04$ s , then the deployment

control process becomes unstable.

TABLE V
SWING AMPLITUDE WITH RESPECT TO THE LOCAL VERTICAL (WITH CONSIDERATION OF THE AERODYNAMIC FORCE)

h ($\mathrm{s}\times10^{-2}$)	1	2	3	4
A (km)	2.31	2.46	2.46	2.22
h ($\mathrm{s}\times10^{-2}$)	4.25	4.5	5	6
A (km)	4.92	10.55	13.36	13.83

In fact, there are a range of uncertainties in the model of atmospheric density. Therefore the simulation results are tested with the change in the atmospheric density ($\pm 20\%$) in the model with distributed parameters (31). It is shown that the simulation results change very little compared with the results in Table II.

In addition, the changes in the orbital inclination, angle β (see Fig. 2), inertia of the control mechanism (m_e) and taking into account the rotation of the atmosphere (41) have little influence on the control errors and swing amplitude.

The form of the tether in the model with distributed parameters (31) during the deployment process is close to straight for all considered cases in this work. Additionally, the tether is divided into ten elements. The number of the tether elements is sufficient, as the increase in the number does not cause any changes in the simulation results.

VIII. CONCLUSION

Based on the analysis of the dynamics of the TSS with the atmospheric sounder, the following conclusions can be drawn:

(1) The nominal deployment control law is designed in the simplified model, in which the tether is treated as a rigid rod. The aerodynamic forces acting on all components of the system are taken into account for designing the nominal control law.

(2) The condition of static stability of the TSS with respect to the local vertical is given as (29). In addition to this, in general cases, the minimum of $|\nu|$ is needed to be obtained when we select parameters of the TSS.

(3) The initial deployment phase is the most dangerous phase for the TSS from the point-of-view of the system's dynamic stability with consideration of the effect of the aerodynamic force. Because in this phase the stabilizing effect of the gravitational moment is minimal.

(4) The signs of the parameters ν and ξ are necessary to be chosen differently. Otherwise, the TSS may lose the motion stability in the initial deployment phase.

(5) Using the nominal deployment program without consideration of the aerodynamic force causes large control error and swing amplitude with respect to the vertical at the end of the deployment.

(6) Taking the aerodynamic force into account for designing the nominal deployment control law can reduce the control error and swing amplitude with respect to the vertical several times.

(7) There is a range for the sampling step, in which the mean control error and the swing amplitude with respect to the vertical are approximately constant. For the case considered in this paper the range is $h \in [0.01\ \mathrm{s}, 0.04\ \mathrm{s}]$.

(8) The above conclusions stay applicable for the changes in the orbital inclination, angle β, inertia of the control mechanism (m_e), and with consideration of the rotation of the atmosphere.

REFERENCES

[1] H. Gläßel, F. Zimmermann, S. Brückner, U. M. Schöttle and S. Rudolph, "Adaptive neural control of the deployment procedure for tether-assisted re-entry," *Aerospace Science and Technology*, vol. 8, pp. 73–81, 2004.

[2] V. S. Aslanov and A. S. Ledkov, "Tether-assisted re-entry capsule deorbiting from an elliptical orbit," *Acta Astronautica*, vol. 130, pp. 180–186, 2017.

[3] S. Cleary and W. J. O' Connor, "Control of Space Debris Using an Elastic Tether and Wave-Based Control," *Journal of Guidance, Control, and Dynamics*, vol. 39, no. 6, pp. 1392–1406, 2016.

[4] K. Hovell and S. Ulrich, "Experimental Validation for Tethered Capture of Spinning Space Debris," in *AIAA SciTech Forum. 2017 AIAA Guidance, Navigation, and Control Conf.*, pp. 2017–1049.

[5] P. Jaworski, V. Lappas, A. Tsourdos, and I. Gray, "Debris Rotation Analysis During Tethered Towing for Active Debris Removal," *Journal of Guidance, Control, and Dynamics*, vol. 40, no. 7, pp. 1769–1778, 2017.

[6] D. V. Elenev and Y. M. Zabolotnov, "Analysis of the Dynamics of the Deployed Aerodynamic Space Tether System," *Cosmic Research*, vol. 55, no. 5, pp. 348–356, 2017.

[7] V. S. Aslanov and R. S. Pikalov, "Rendezvous of Non-Cooperative Spacecraft and Tug Using a Tether System," *Engineering Letters*, vol. 25, no. 2, pp. 142–146, 2017.

[8] M. B. Quadrelli, M. Ono, and A. Jain, "Modeling of Active Tether System concepts for planetary exploration," *Acta Astronautica*, vol. 138, pp. 512–529, 2017.

[9] V. V. Beletsky and E. M. Levin, *The dynamics of space tether systems*. Moscow: Science Publ, 1990, pp. 336.

[10] H. Troger, A. P. Alpatov, V. V. Beletsky, V. I. Dranovskii, V. S. Khoroshilov, A. V. Pirozhenko, and A. E. Zakrzhevskii, *Dynamics of Tethered Space Systems*. FL: CRC Press, 2010, pp. 245.

[11] V. S. Aslanov and A. S. Ledkov, *Dynamics of Tethered Satellite Systems*. Woodhead Publishing, 2012, pp. 256.

[12] M. L. Cosmo and E. C. Lorenzini, *Tethers in Space Handbook, 3rd Ed*. NASA Marshall Space Flight Center, Huntsville, 1997, pp 241.

[13] B. S. Yu, D. P. Jin, and H. Wen, "Analytical deployment control law for a flexible tethered satellite system," *Aerospace Science and Technology*, vol. 66, pp. 294–303, 2017.

[14] P. Williams, "Optimal deployment/retrieval of a tethered formation spinning in the orbital plane," *Journal of Spacecraft and Rockets*, vol. 43, no. 3, pp. 638–650, 2006.

[15] A. Steindl, "Optimal control of the deployment (and retrieval) of a tethered satellite under small initial disturbances," *Meccanica*, vol. 49, no. 8, pp. 1879–1885, 2014.

[16] P. Williams, "Electrodynamic Tethers Under Forced–Current Variations Part 2: Flexible–Tether Estimation and Control," *Journal of Guidance, Control, and Dynamics*, vol. 47, no. 2, pp. 320–333, 2010.

[17] H. T. K. Linskens and E. Mooij, "Tether Dynamics Analysis for Active Space Debris Removal," in *AIAA SciTech Forum. 2016 AIAA Guidance, Navigation, and Control Conf.*, pp. 2016–1129.

[18] Y. M. Zabolotnov, "Control of the deployment of a tethered orbital system with a small load into a vertical position," *Journal of Applied Mathematics and Mechanics*, vol. 79, no. 1, pp. 28–34, 2015.

[19] M. Kruijff, *Tethers in Space*. The Netherlands: Delta - Utec Space Research, 2011, pp. 432.

[20] M. Liu, X. Q. Zhan, Z. H. Zhu, and B. Y. Liu, "Space Tether Deployment with Explicit Non-Overshooting Length and Positive

Velocity Constraints," *Journal of Guidance, Control, and Dynamics*, vol. 40, no. 12, pp. 3310–3315, 2017.
[21] Z. Q. Cai, X. F. Li, and Z. G. Wu, "Deployment and retrieval of a rotating triangular tethered satellite formation near libration points," *Acta Astronaut*, vol. 98, no. 1, pp. 37–49, 2014.
[22] P. Williams, A. Hyslop, M. Stelzer, and M. Kruijff, "YES2 optimal trajectories in presence of eccentricity and aerodynamic drag," *Acta Astronautica*, vol. 64, pp. 745–769, 2009.
[23] K. D. Kumar, "Review of Dynamics and Control of Nonelectrodynamic Tethered Satellite Systems," *Journal of Spacecraft and Rockets*, vol. 43, no. 4, pp. 705–720, 2006.
[24] A. K. Misra, "Dynamics and control o f tethered satellite systems," *Acta Astronautica*, vol. 63, pp. 1169–1177, 2008.
[25] V. S. Aslanov, "Oscillations of a spacecraft with a vertical tether," *Proceedings of the World Congress on Engineering 2009 Vol II WCE 2009*, July 1 - 3, 2009, London, U.K.
[26] S. P. Bezglasnyi, "Bounded parametric control of space tether systems motion," *Lecture Notes in Engineering and Computer Science: Proceedings of The World Congress on Engineering 2017*, 5-7 July, 2017, London, U.K., pp. 76-79.
[27] Y. M. Zabolotnov, "Control of the Deployment of an Orbital Tether System That Consists of Two Small Spacecraft," *Cosmic Research*, vol. 55, no. 3, pp. 224–233, 2017.
[28] M. Kruijff, E. J. van der Heide, W. J. Ockels, and E. Gill, "First Mission Results of the YES2 Tethered SpaceMail Experiment," in *AIAA/AAS Astrodynamics Specialist Conf. and Exhib., 2008*, pp. 2008–7385.
[29] G. S. Narimanov and M. K. Tikhonravov, *Fundamental of the theory of flight spacecraft*, Moscow: Mashinostroenie, 1972, pp. 608 (in Russian).
[30] Z. Dong, Y. M. Zabolotnov and C. Q. Wang, "Analysis of motion stability of a deployed space tether system with an atmospheric probe," *Vestnik of Samara University. Aerospace and Mechanical Engineering*, vol. 15, no. 2, pp. 102–113, 2016 (in Russian).
[31] N. S. Arzhannikov and G. S. Sadekova, *Aerodynamics of aircrafts*, Vysshaya shkola Publishers, Russia, 1983, pp. 360 (in Russian).
[32] GOST R 25645.166 – 2004 Earth upper atmosphere. Density model for ballistic support of flights of artificial earth satellites (National Standard of Russian Federation). Standard form. Moscow, 2004.
[33] Y. M. Zabolotnov, *Intoduction to Dynamics and Control in Space Tether System*. Beijing: Science Press, 2013, pp. 140 (in Chinese).